



**SQUARE KILOMETRE ARRAY**  
百万平米電波望遠鏡

# Exploring the Diffuse Ionized Gas in Our Galaxy by means of Long Wavelength Radio Observation (2016 Edition)



**Takuya AKAHORI**

**Kagoshima University, Japan**

SKA-Japan Project A/Prof. | SKA-Japan Vice Chair |  
SKA Cosmic Magnetism SWG

The 6th DTA Symposium 2016  
16.11.24-25 @ NAOJ, Mitaka

- ❖ **Introduction**
- ❖ **Magnetized diffuse ionized gas (DIG) in the Galaxy**
  - Thermal electrons
  - Magnetic fields
    - Global magnetic fields
    - Magnetic turbulence
  - Cosmic-rays
- ❖ **Toward Square Kilometre Array (SKA)**
  - Specification
  - Possible application?
    - Star-forming region
    - Jet terminal shock
    - Dense molecular gas

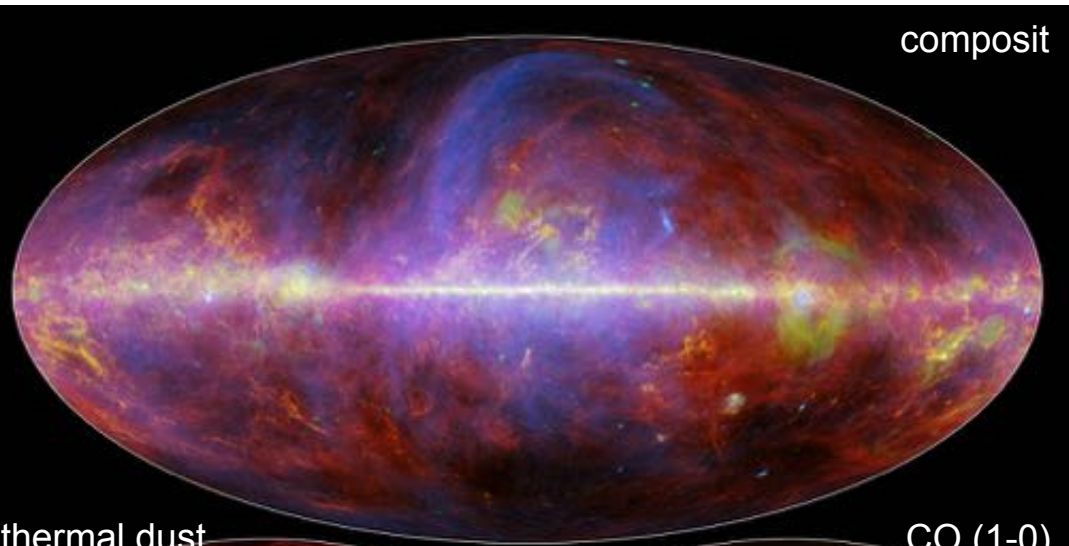
## お題

- 近年の銀河磁場の観測
- SKA計画で目指すサイエンス

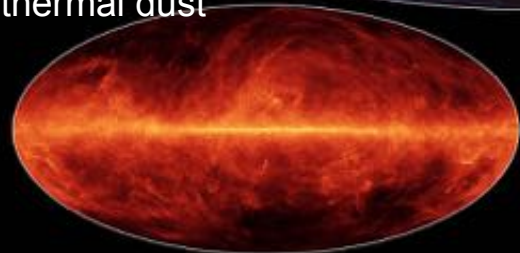
大スケールの銀河磁場と小スケールの分子雲磁場がどのように関連するかといった点

# 1. Introduction

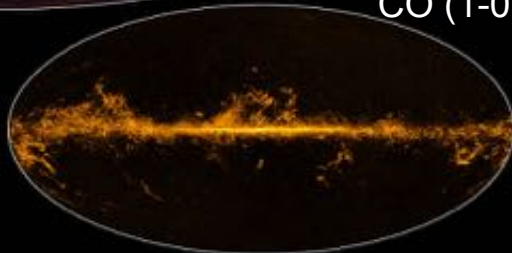
## Radio Milky Way



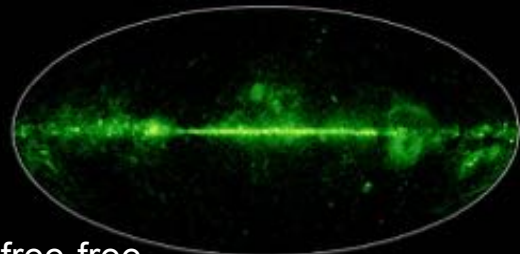
thermal dust



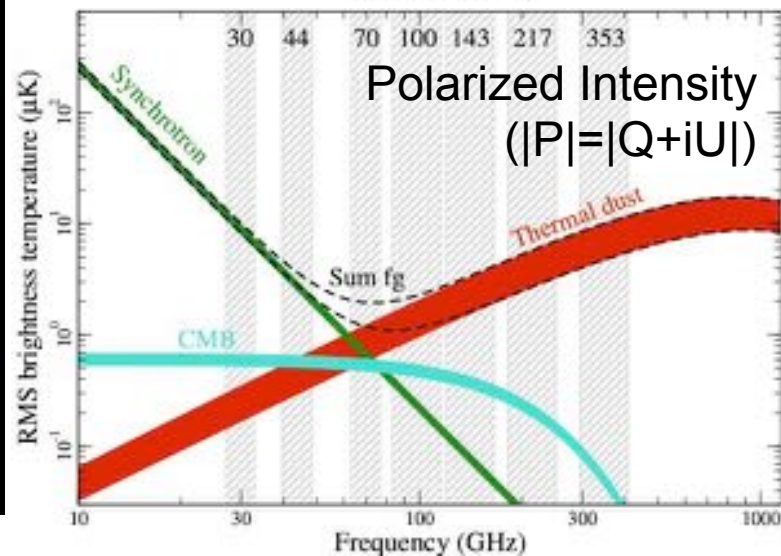
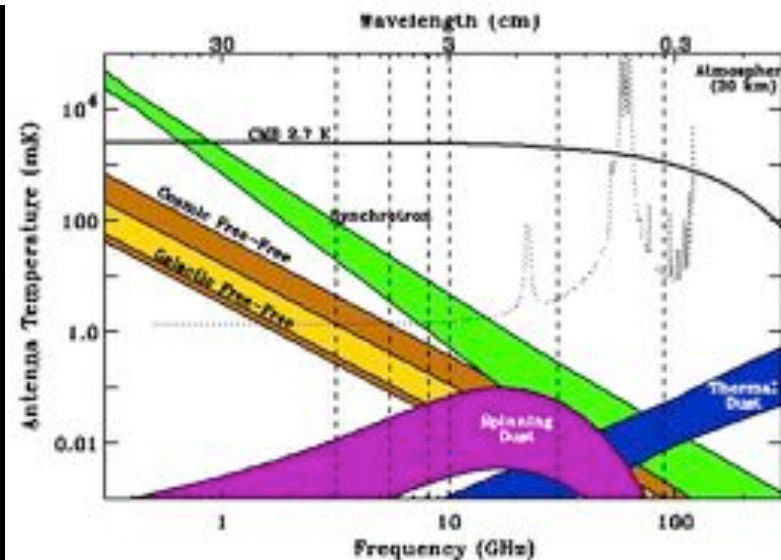
CO (1-0)



free-free



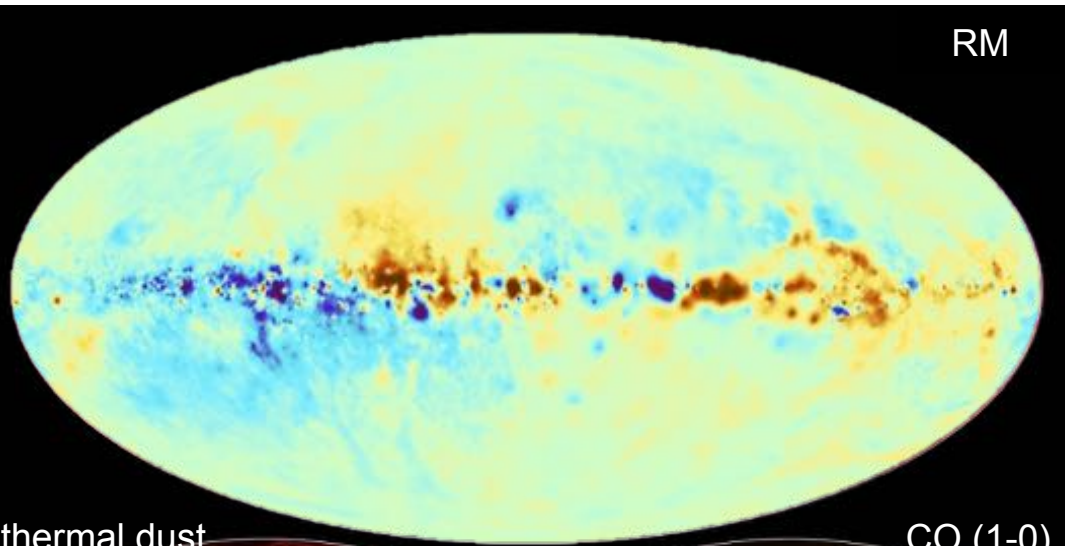
synchrotron



<https://www.nasa.gov/jpl/planck/pia18913>

# 1. Introduction

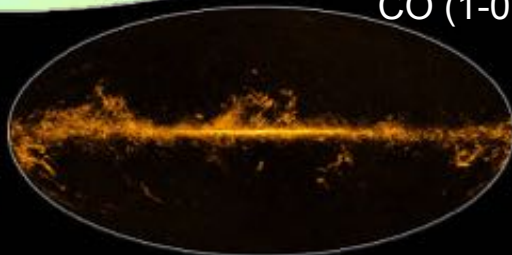
## Radio Milky Way



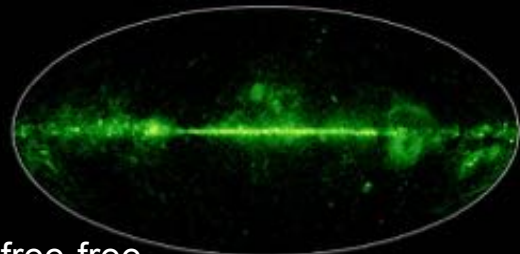
thermal dust



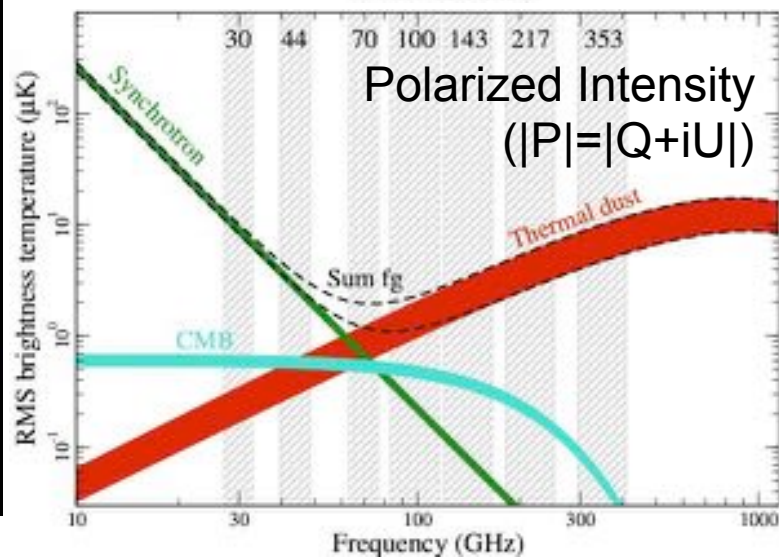
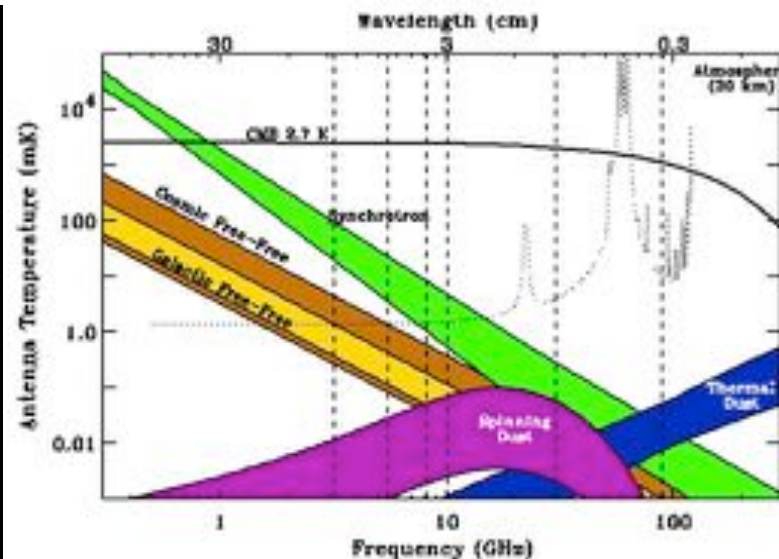
CO (1-0)



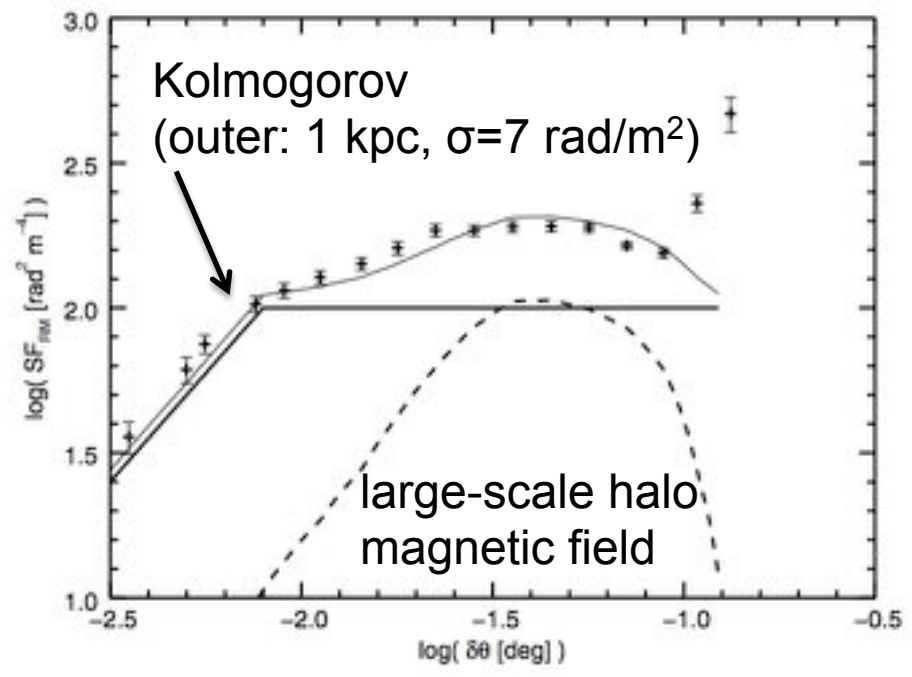
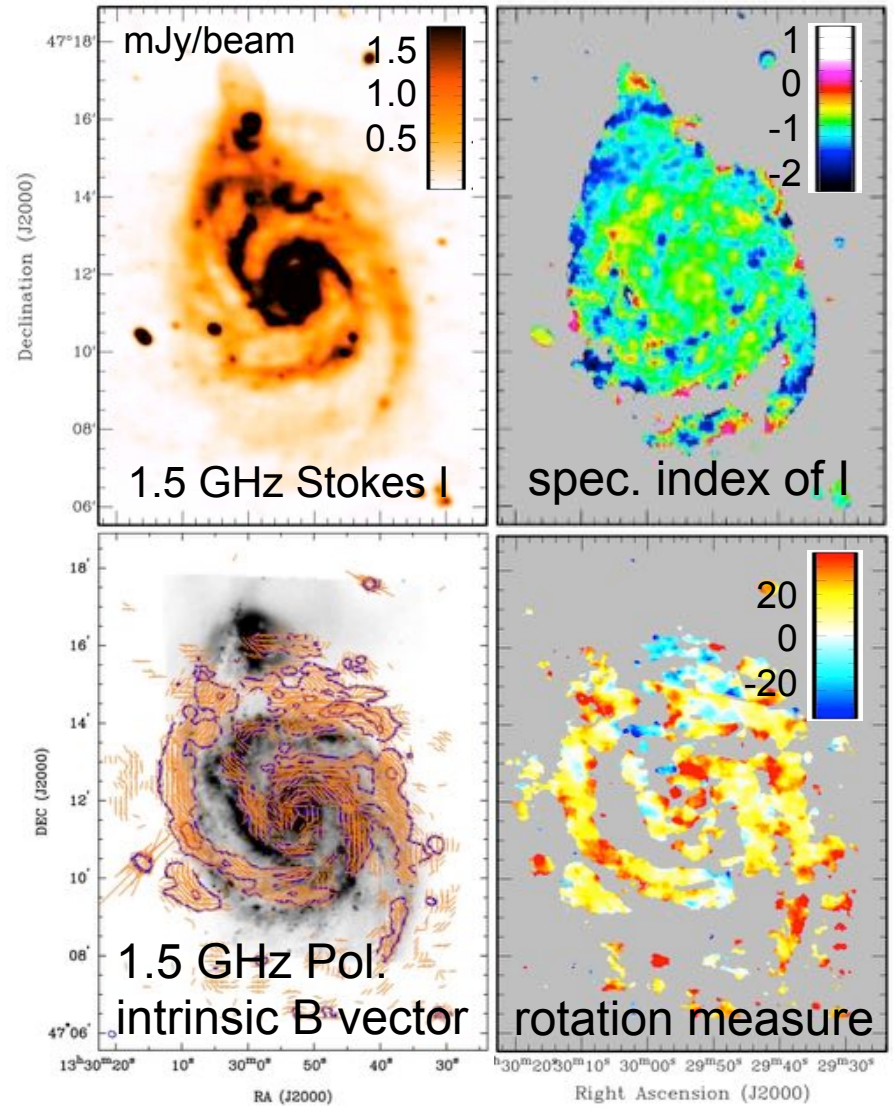
free-free



synchrotron



<https://www.nasa.gov/jpl/planck/pia18913>



❖ **Long wavelength radio (centimeter – meter) is a very powerful tool for magnetism.**

## ❖ Pulsars and Fast Radio Bursts (FRBs)

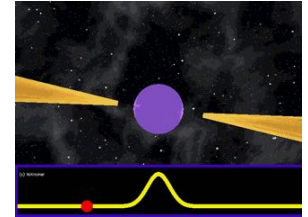
– Pulse dispersion → **dispersion measure (DM)**

- pulse delay time  $\Delta t$

$$\Delta t \text{ (msec)} \simeq 4.2 \left( \frac{DM}{\text{pc cm}^{-3}} \right) \left( \frac{\nu}{\text{GHz}} \right)^{-2}$$

$n_e$ : free electron density

$$DM = \int_0^L n_e dl$$



– Diffractive (幾何光学) / refractive (物理光学) scintillations

→ **scattering measure (SM)**

- pulse modulation time  $\Delta t$

$C_N$ : spectral coefficient of the density power spectrum

$$\Delta t \text{ (msec)} \simeq 1.1 \left( \frac{SM}{\text{kpc m}^{-20/3}} \right)^{6/5} \left( \frac{L}{\text{kpc}} \right) \left( \frac{\nu}{\text{GHz}} \right)^{-22/5} \quad SM = \int_0^L C_N^2 dl$$

–  $\langle n_e \rangle \sim DM/L$ , or  $\langle n_e^2 \rangle \sim SM/L$

- L: distance (e.g. by annual parallax)

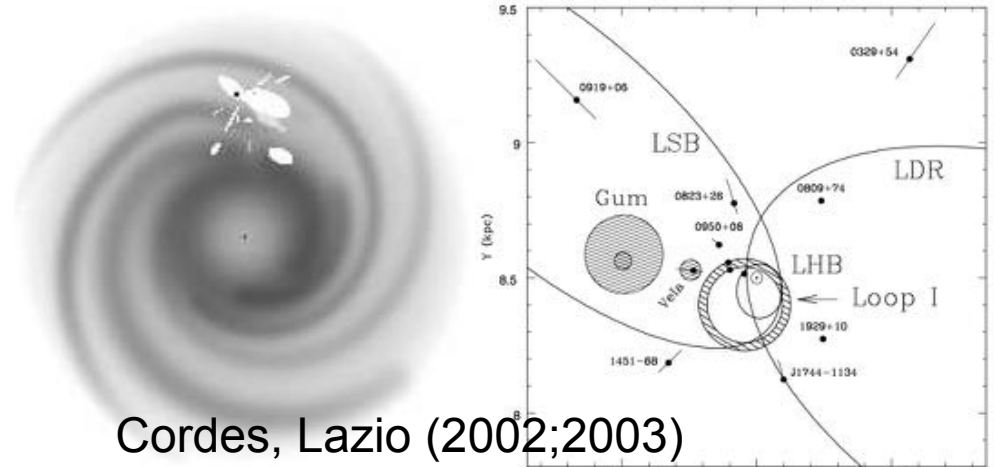
## ❖ NE2001 model

- Analytical model of the thermal electron density based on observations
- Components: thick disk, thin disk, arm, local, clumps, voids

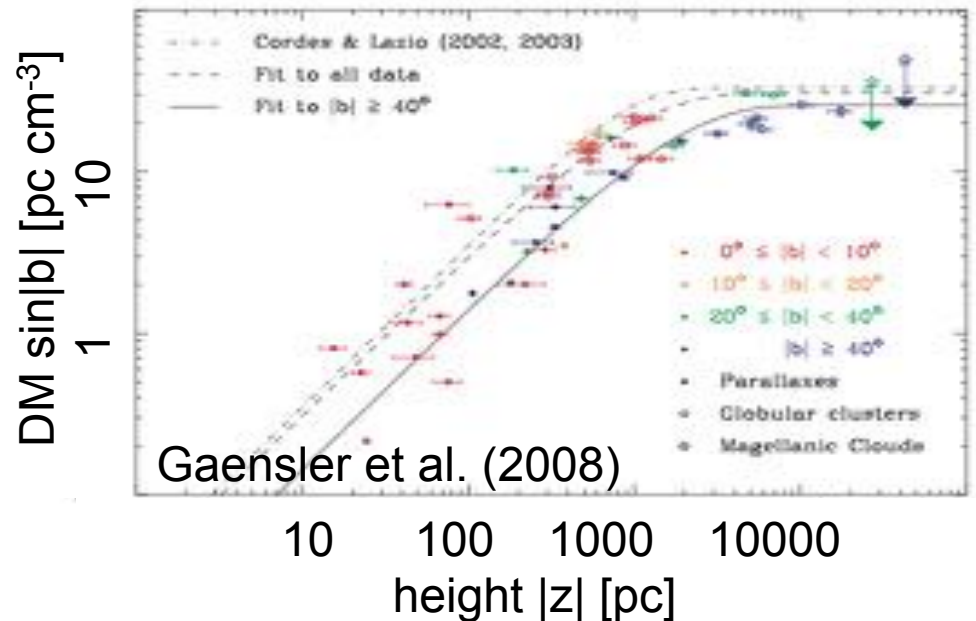
## ❖ Scale height

$$n(z) = n_0 \exp\left(-\frac{z}{H_n}\right)$$

- $H_n$  too small in NE2001
- $H_n = 0.97 \text{ kpc} \rightarrow 1.8 \text{ kpc}$
- $n_0 \rightarrow 0.014 \text{ cm}^{-3}$



Cordes, Lazio (2002;2003)



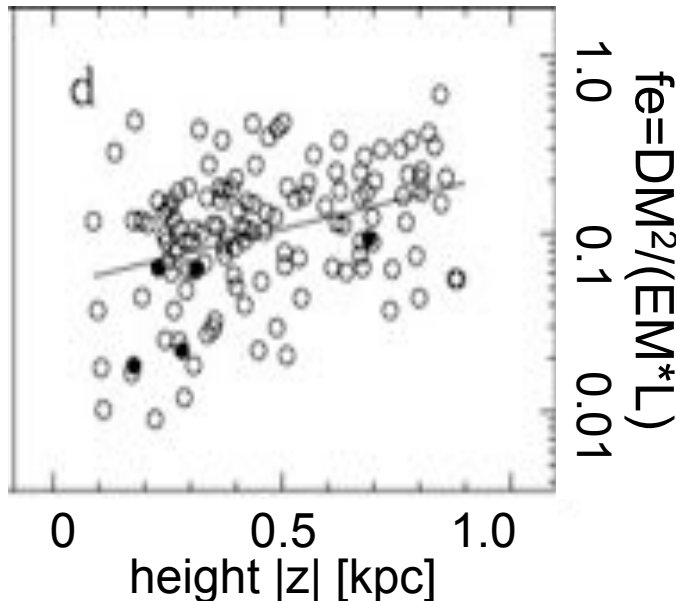
Gaensler et al. (2008)

# Clumpiness and filling factor

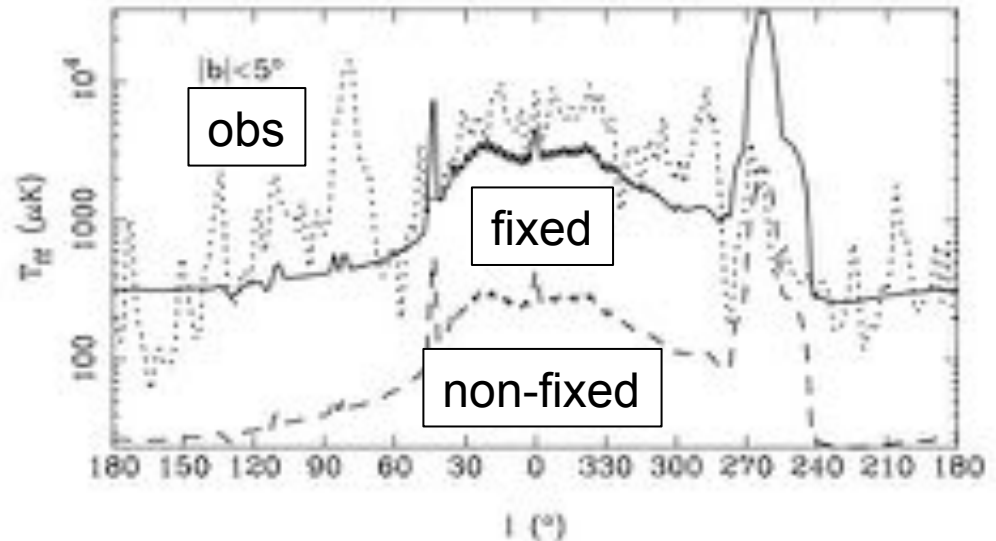
## ❖ DM gives the average of thermal electron density

- Electron distribution is **clumpy**
- Need the filling factor to reproduce free-free emission

$$EM = \int_0^L n_e^2 dl \quad f_e = \frac{\langle n_e \rangle^2}{\langle n_e^2 \rangle} = 0.07 \exp\left(\frac{|z|}{0.5 \text{ kpc}}\right) \text{ or } 0.32 (|z| > 0.75 \text{ kpc})$$



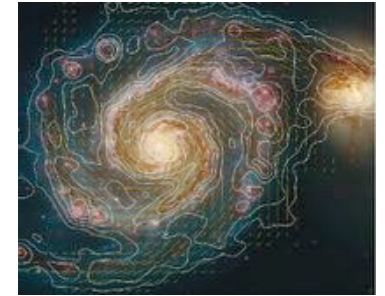
Berkhuijsen et al. (2006)



dotted: 22.8GHz free-free template data  
dashed: w/o filling factor, solid: w/ filling factor  
Sun et al. (2008)



### ❖ Faraday rotation measure of background sources



– Faraday rotation → **rotation measure (RM)**

- Rotation of polarized angle  $\Delta\Phi$

$$\Delta\Phi \text{ (rad)} \simeq 0.318\pi \left( \frac{\text{RM}}{\text{rad m}^{-2}} \right) \left( \frac{\lambda}{1 \text{ m}} \right)^2$$

$B_{\parallel}$ : line-of-sight component of magnetic field

$$\text{RM} = \int_L n_e B_{\parallel} dl$$

– Depolarization → **dispersion of RM ( $\sigma_{\text{RM}}$ )**

- Degree of internal/external Faraday rotation depolarization  $\text{DPi}/\text{DPe}$

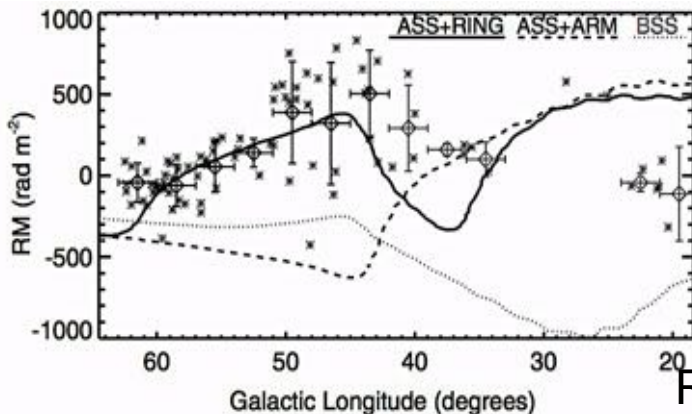
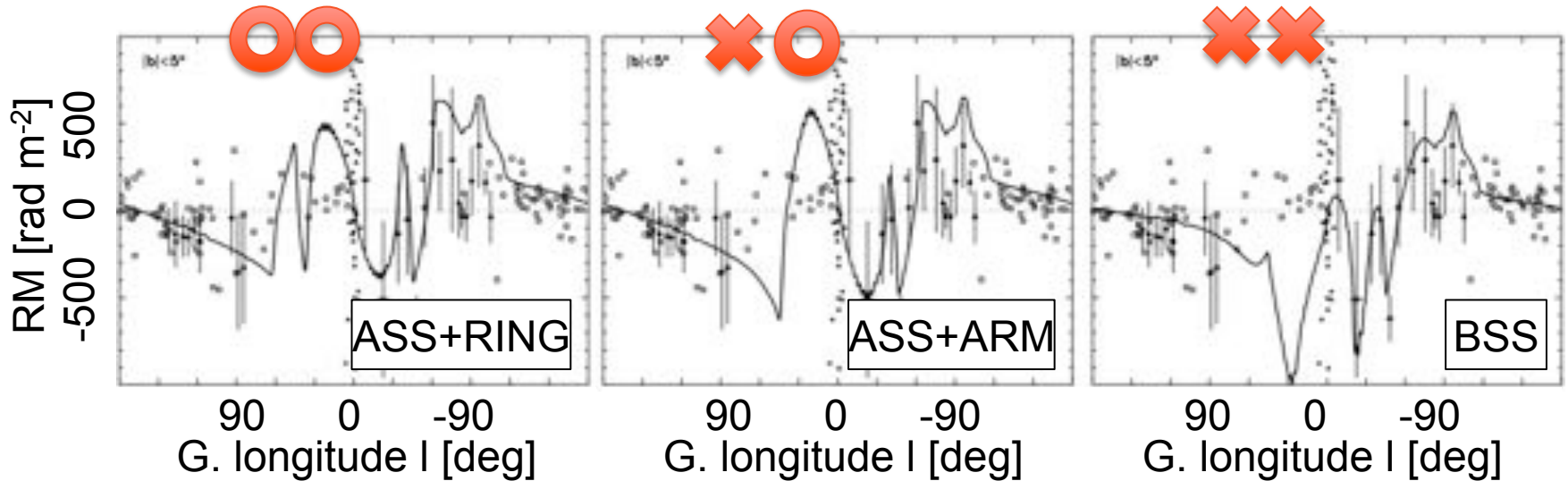
$$\text{DPi} = \frac{1 - \exp(-2\sigma_{\text{RM}}^2 \lambda^4)}{2\sigma_{\text{RM}}^2 \lambda^4}$$

$$\text{DPe} = \exp(-2\sigma_{\text{RM}}^2 \lambda^4)$$

–  **$\langle B_{\parallel} \rangle \sim \text{RM}/\text{DM}$**

### ❖ Axi-Symmetric Spiral (ASS) vs. Bi-Symmetric Spiral (BSS)

– ASS + reversal,  $B_0 \sim 2-6 \mu\text{G}$  (Sun et al. 2008; Van Eck et al. 2011)



RM (CGPS+SGPS,  $|b| < 5^\circ$ ) Lines: model (Sun+ 2008)

$$\begin{cases} B_{s,R}(R, \Theta, z) = D_1(R, z)D_2(R, \Theta) \sin(p_{s0}), \\ B_{s,\Theta}(R, \Theta, z) = -D_1(R, z)D_2(R, \Theta) \cos(p_{s0}), \\ B_{s,z}(R, \Theta, z) = 0, \end{cases} \quad D_1(R, z) = \begin{cases} B_{s0} \exp\left(-\frac{R-R_\odot}{R_{s0}} - \frac{|z|}{z_{s0}}\right) & R > R_{sc}, \\ B_{sc} \exp\left(-\frac{|z|}{z_{sc}}\right) & R \leq R_{sc}. \end{cases}$$

$$D_2(R, \Theta) = \begin{cases} +1 & R > 7.5 \text{ kpc}, \\ -1 & 6 \text{ kpc} < R \leq 7.5 \text{ kpc}, \\ +1 & 5 \text{ kpc} < R \leq 6 \text{ kpc}, \\ -1 & R \leq 5 \text{ kpc}, \end{cases} \quad D_2(R, \Theta) = \sin\left(\Theta + \frac{1}{\tan p_{s0}} \ln \frac{R}{R_{sb}}\right)$$

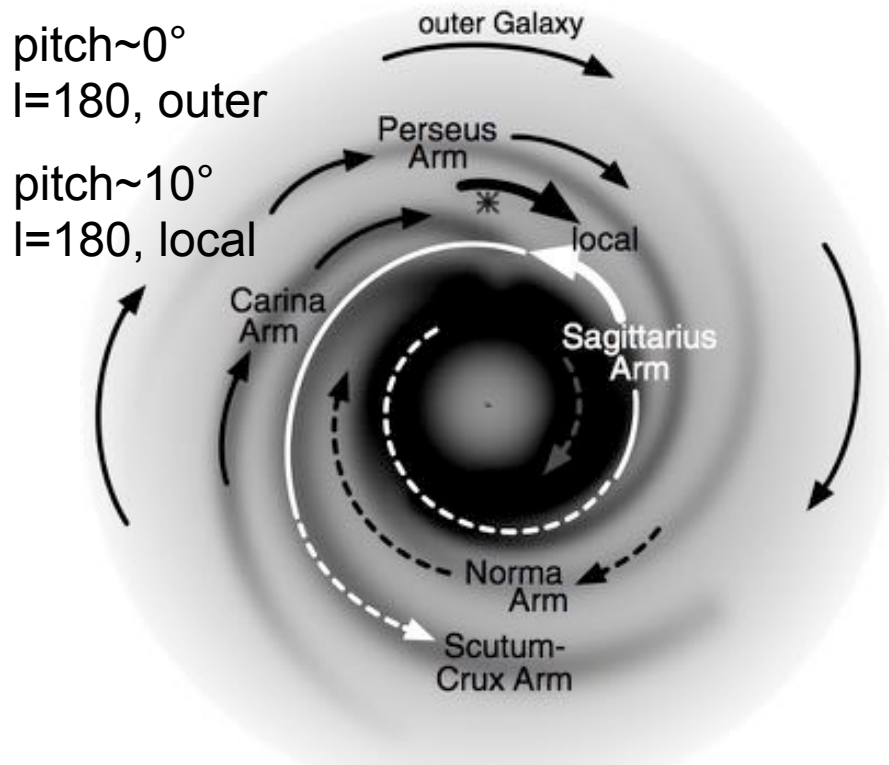
RM data (NVSS+CGPS,  $|b| < 3^\circ$ )

Lines: model (Van Eck et al. 2011)

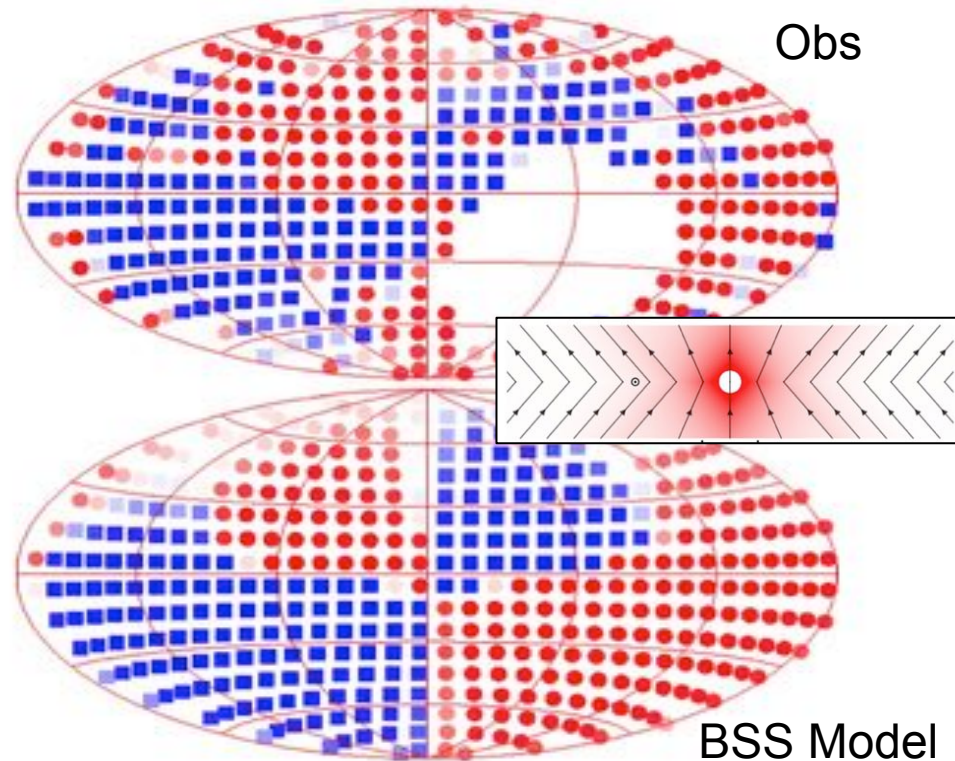
### ❖ ASS to BSS transition at mid galactic latitudes?

- ASS-RING in the galactic disk, BSS in halo\*\*
- Effect of vertical (X-shape) field?

\*\*M51  
ASS in disk  
BSS in halo



Van Eck et al. (2011)

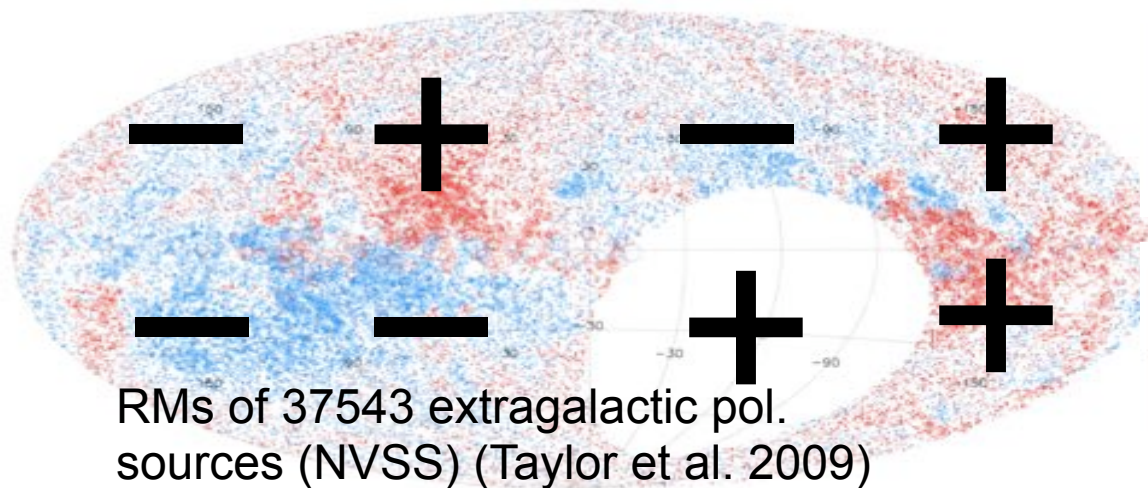


Pshirkov et al. (2011)

BSS Model

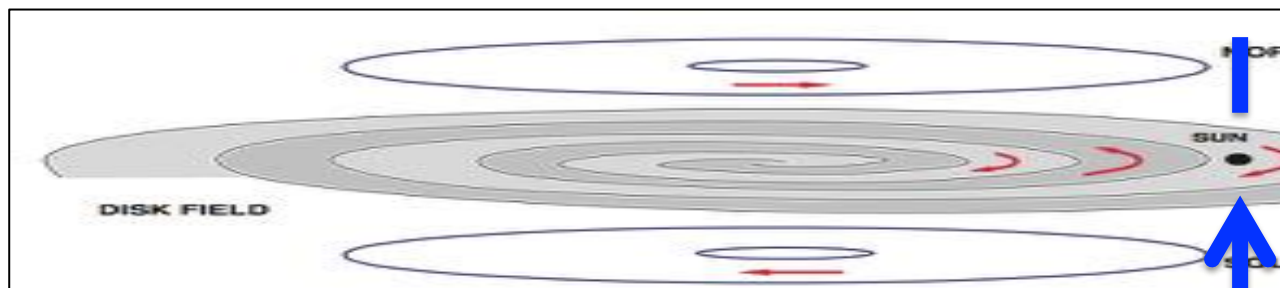
### ❖ Toroidal field (~2 μG) + vertical field near the Sun

- inner: galactic-center symmetry, outer: galactic-axis symmetry (Taylor et al. 2009; Oppermann et al. 2011)
- **vertical field** toward only south galactic pole (Mao et al. 2010)



$$\begin{cases} B_{t,R}(R, \Theta, z) = 0, \\ B_{t,\Theta}(R, \Theta, z) = \frac{\text{sign}(z)^v B_{t0}}{1 + \left(\frac{|z| - z_{t0}}{z_{t1}}\right)^2} \frac{R}{R_{t0}} \exp\left(-\frac{R - R_{t0}}{R_{t0}}\right) \\ B_{t,z}(R, \Theta, z) = 0, \end{cases}$$

$$\begin{cases} B_{x,R}(R, \Theta, z) = \text{sign}(z) B_{x0} \exp\left(-\frac{R_p}{R_{x0}}\right) \left(\frac{R_p}{R}\right)^w \cos \eta, \\ B_{x,\Theta}(R, \Theta, z) = 0, \\ B_{x,z}(R, \Theta, z) = B_{x0} \exp\left(-\frac{R_p}{R_{x0}}\right) \left(\frac{R_p}{R}\right)^w \sin \eta. \end{cases}$$



RM ~ +0.0 ± 0.5 rad/m<sup>2</sup>  
B<sub>||</sub> ~ 0.00 ± 0.02 μG

Mao et al. (2010)

RM ~ +6.3 ± 0.5 rad/m<sup>2</sup>  
B<sub>||</sub> ~ 0.31 ± 0.02 μG

### ❖ Power spectrum, $P \sim k^{-\beta}$

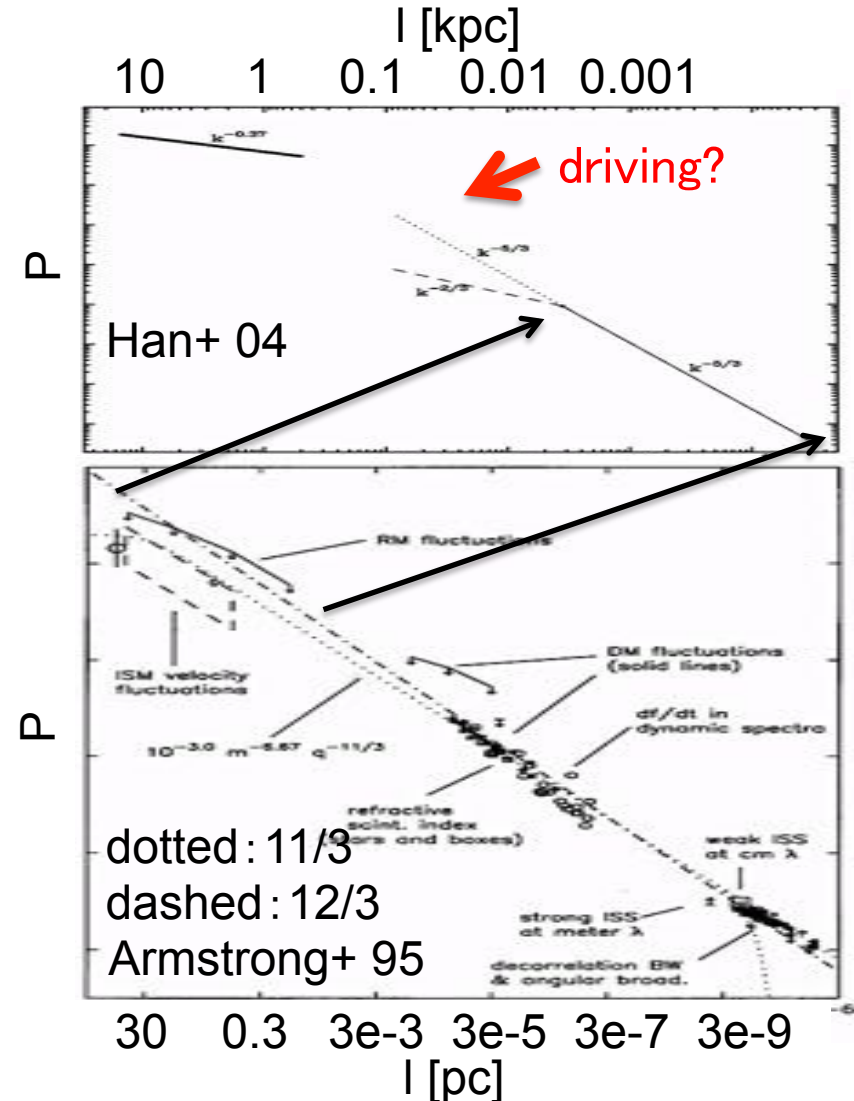
- Kolmogorov ( $\beta=5/3$ ) (Armstrong et al. 1995)
- Outer scale of  $> \sim 1$  kpc ( $\beta=0.37$ ) (Han et al. 2004)
- Amplitude: 3-5  $\mu\text{G}$  at disk

### ❖ Driving scale

- $\sim 1$  pc @ spiral-arms
- $\sim 100$  pc @ inter-arms (Haverkorn et al. 2008)

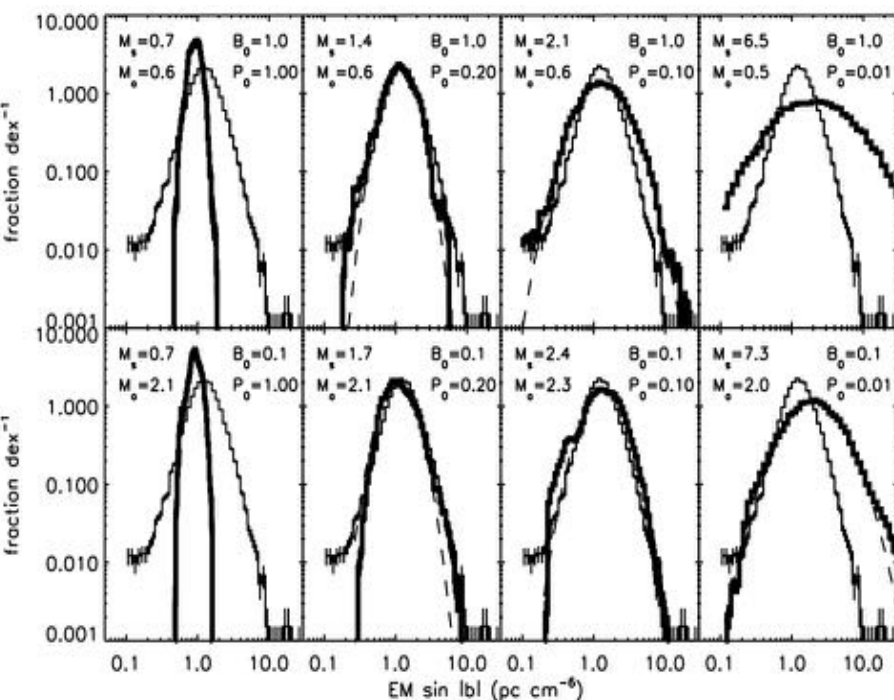
### ❖ Remarks

- Ordered fields (Jaffe et al. 2010)

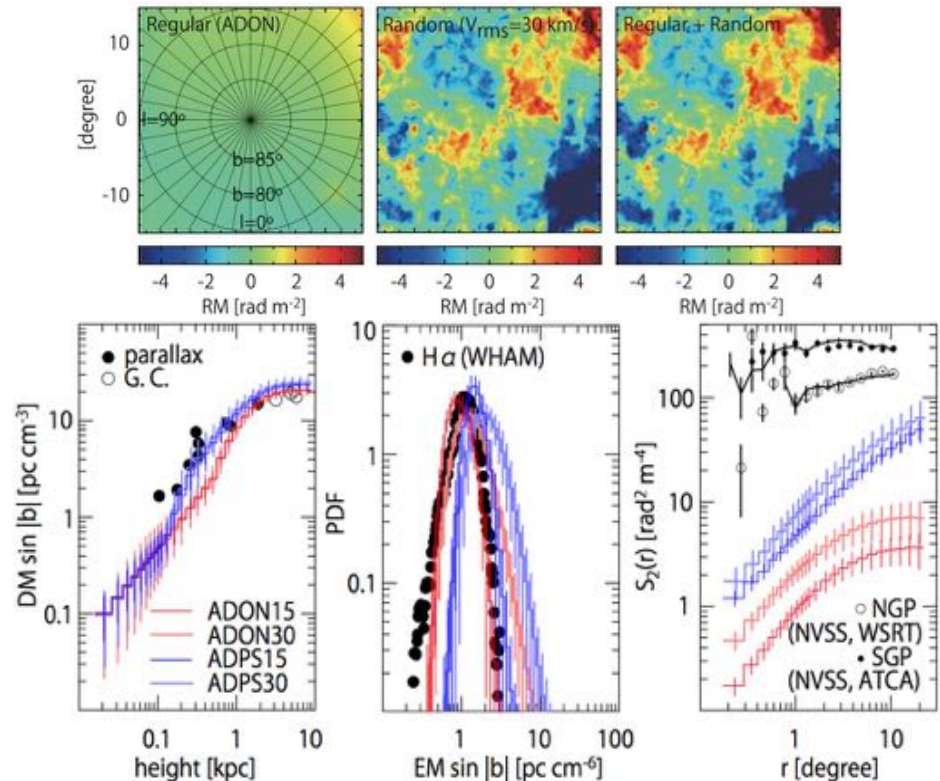


### ❖ Mach number $M$ , plasma $\beta$ , and driving scale

- EM + MHD  $\rightarrow M \sim 1.4-2.4$ ,  $l_{\text{drive}} \sim 500 \text{ pc}$  (Hill et al. 2008)
- DM + EM +  $\langle \text{RM} \rangle$  + MHD  $\rightarrow \beta \sim 0.1-1$ ,  $\sigma_{\text{RM}} \sim \text{few rad/m}^2$



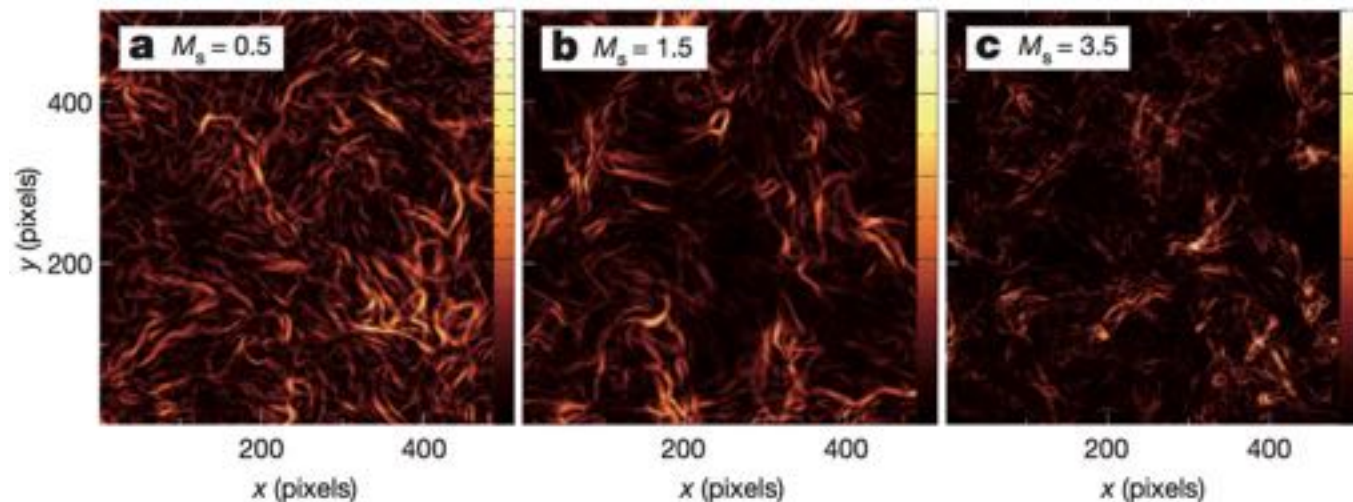
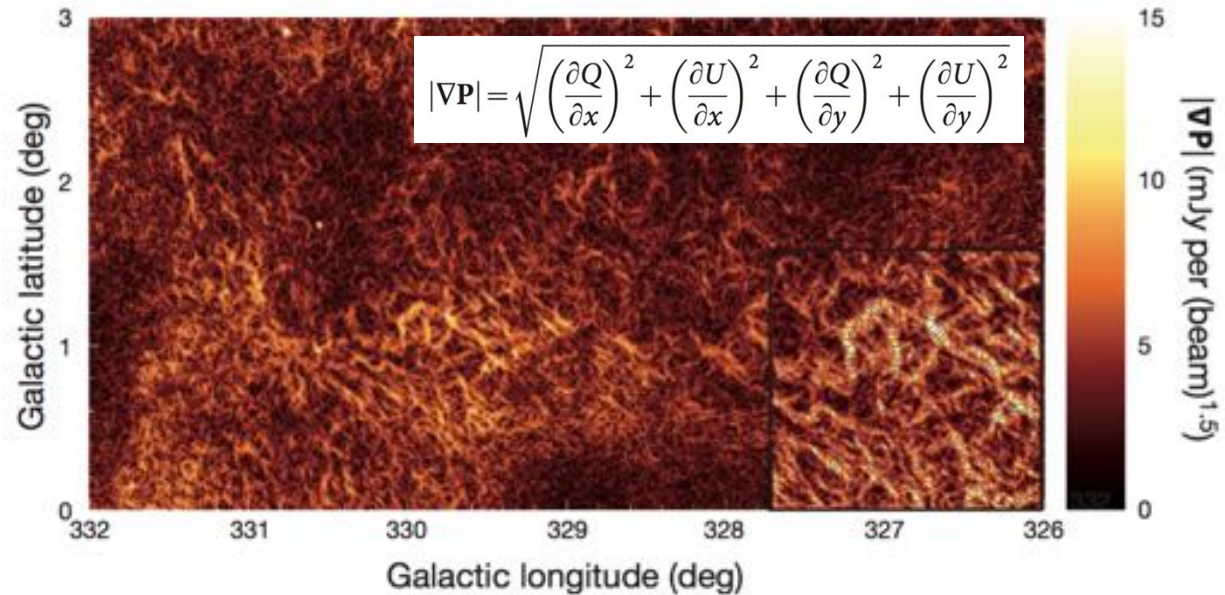
thin: observation, thick: MHD model  
Hill et al. (2008)



Akahori et al. (2013)

### ❖ Polarization gradient $\nabla P$ unveils the Mach number

- Gaensler et al. (2011)
- prefer  $M < 2$



❖ **Alfven velocity (in SI):**

$$v_A = \frac{B}{\sqrt{\mu_0 \rho}}$$

❖ **Rotation measure:**

$$\phi = 2.63 \times 10^{-13} (\mu_e m_p)^{1/2} \mu_0^{1/2} \int n_e^{3/2} \frac{B_{\parallel}}{\sqrt{\mu_0 \rho}} L dx.$$

❖ **Density-weighted Alfven velocity:**

$$\bar{v}_A = \frac{\int n_e^{3/2} v_A dl}{\int n_e^{3/2} dl} \quad \bar{v}_A \geq \left[ \frac{(\mu_e m_p)^{-1/2} \mu_0^{-1/2}}{2.63 \times 10^{-13}} \right] \frac{|\phi|}{\int n_e^{3/2} dl}$$

❖ **Dimensionless factor R**

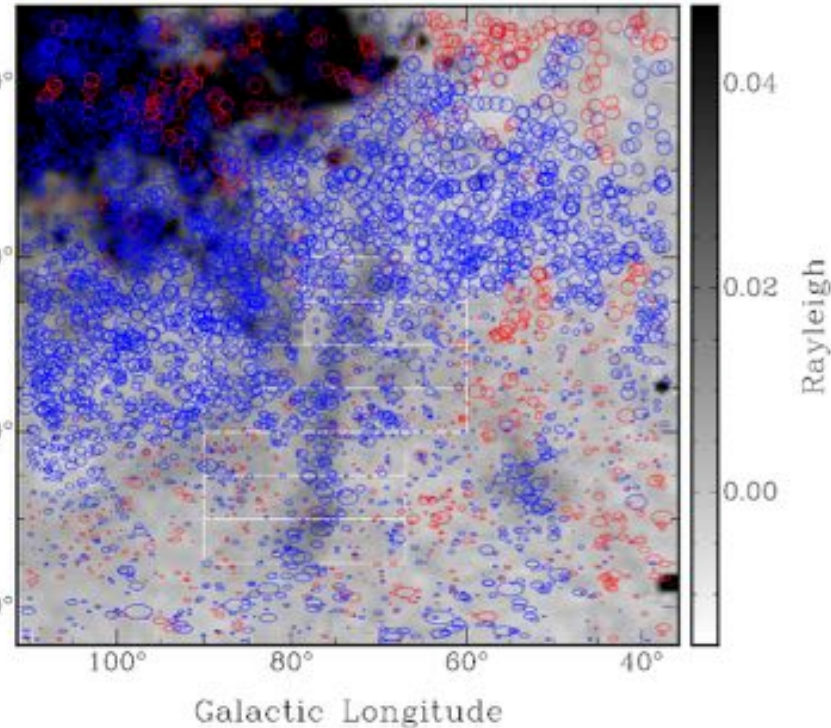
– R=1 uniform density, R=1.0755 gaussian

$$\mathcal{R} \equiv \frac{\int n_e^{3/2} dx}{\left[ \int n_e^2 dx \right]^{3/4}} = f^{-1/4} L^{-1/4} \frac{\int n_e^{3/2} dl}{EM^{3/4}}$$

$$\bar{v}_A \geq (0.820 \text{ km s}^{-1}) \mu_e^{-1/2} f^{-1/4} \times \left( \frac{L}{100 \text{ pc}} \right)^{-1/4} \mathcal{R}^{-1} \left[ \frac{|\phi|}{EM^{3/4}} \right]$$

❖ **Sound speed & plasma  $\beta$ :**

$$c_S = \left( \frac{kT}{\mu m_H} \right)^{1/2} = (8.12 \text{ km s}^{-1}) \mu^{-1/2} \left( \frac{T}{8000 \text{ K}} \right)^{1/2} \quad \beta = \frac{p_t}{p_B} = \frac{c_S^2}{v_A^2}$$



$H_{\alpha}$  at  $V_{\text{LSR}} = -45 \text{ km/s}$ ,  
Extragalactic  $|RM|$  max  $70 \text{ rad/m}^2$

❖  **$\beta < \sim 1$  in the filaments**

–  $\beta < \sim 0.1$  at  $b \sim 50^\circ$



❖ **Cosmic-ray electrons (CRe):**  $N(\gamma)d\gamma = N_0\gamma^{-p}d\gamma$

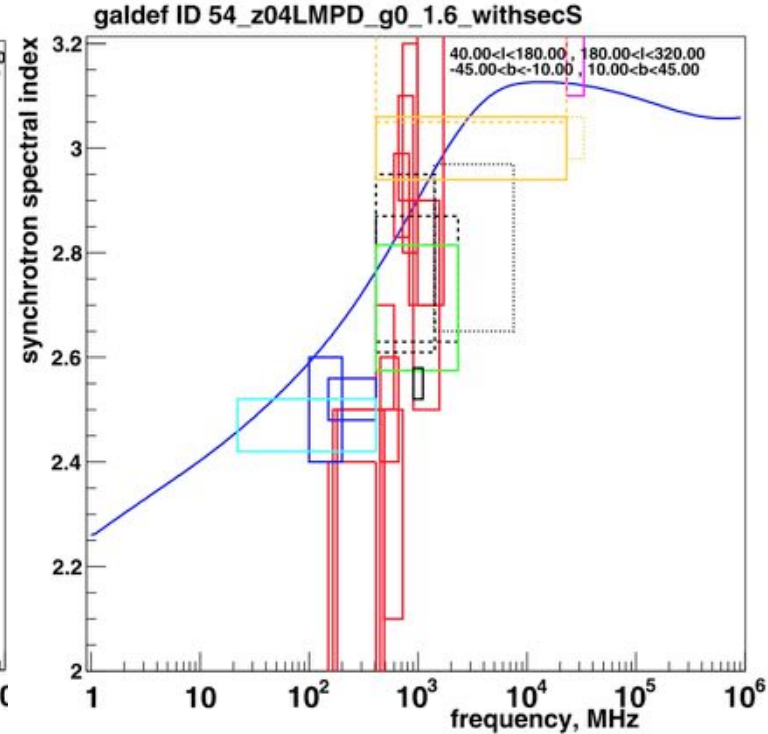
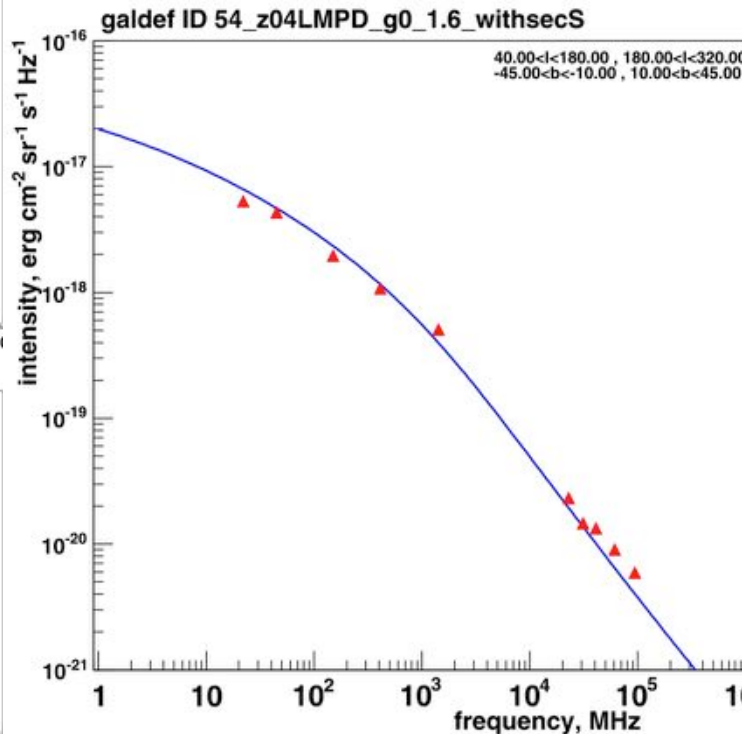
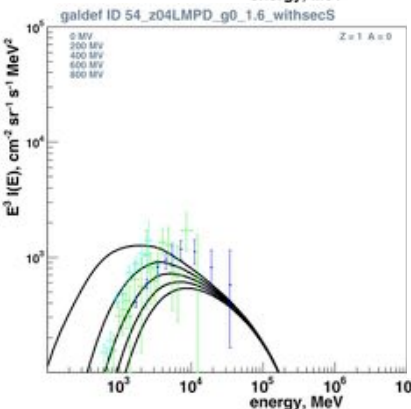
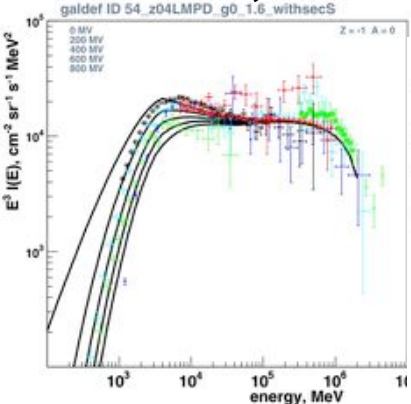
–  $p \sim 2.5-3$  @  $\sim 3-30$  GeV CRe

AMS01, CAPRICE, HEAT, Fermi-LAT,  
PAMELA, ATIC-1-2, HESS

$N_0$ : CRe density normalization ( $\text{cm}^{-3}$ )

$\gamma$ : Lorentz factor

$p$ : energy spectral index



### ❖ CRe + B = **Synchrotron**

– Specific stokes I, Q, U

$$I \propto n_c B_{\parallel}^{(1+p)/2} \omega^{(1-p)/2}$$

$$Q + iU \propto n_c B_{\parallel}^{(1+p)/2} \omega^{(1-p)/2} e^{-2i\chi}$$

$B_{\parallel}$ : LoS component of magnetic field [ $\mu\text{G}$ ]

$\omega$ :  $2\pi\nu$ ,  $\chi$ : intrinsic polarization angle ( $\perp B_{\perp}$ )

– Spectral index  $I \propto \nu^{\alpha}$

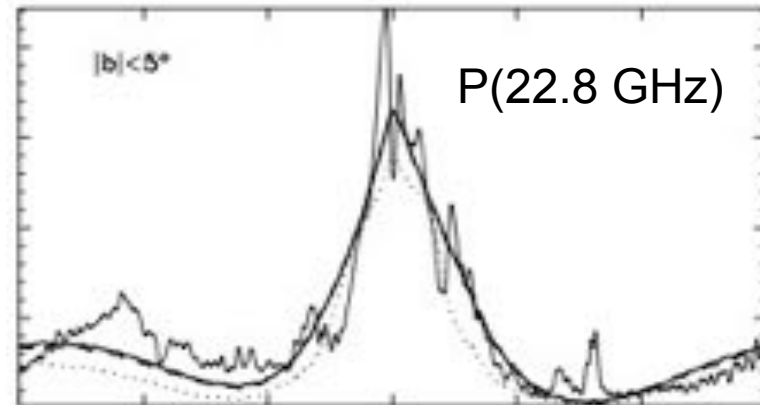
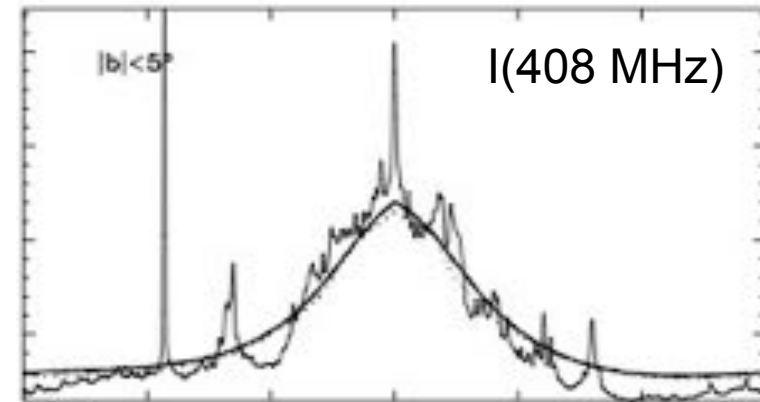
- $\alpha = (1-p)/2$

### ❖ Spatial distribution of CRe

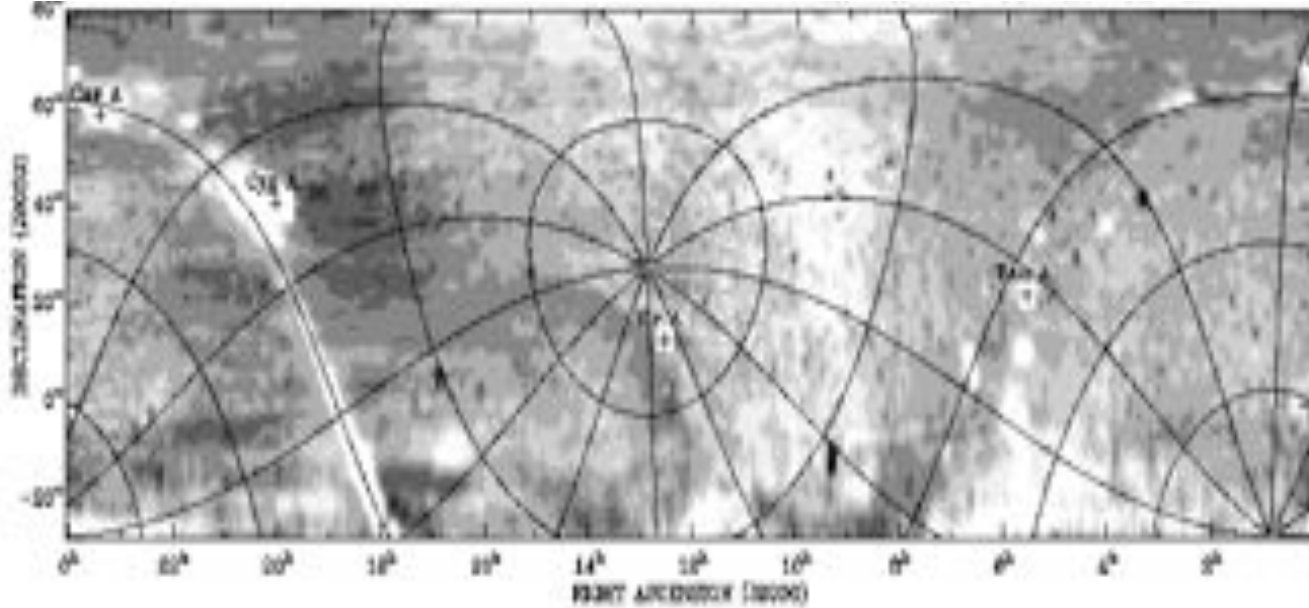
–  $n_{c0} = 5 \times 10^{-5} \text{ cm}^{-3}$ ,  $H_c = 0.8 \text{ kpc}$

$$n_c(R, z) = n_{c0} \exp\left(-\frac{R - R_{\odot}}{8 \text{ kpc}} - \frac{|z|}{H_c}\right)$$

dashed: I, P data ( $|b| < 5^{\circ}$ )  
 solid: model (Sun et al. 2008)



90 0 -90  
galactic longitude  $l$  [deg]



$p$  2.3 2.4 2.5 2.6

Spectral index map  
at 22 MHz  
(Roger et al. 1999)

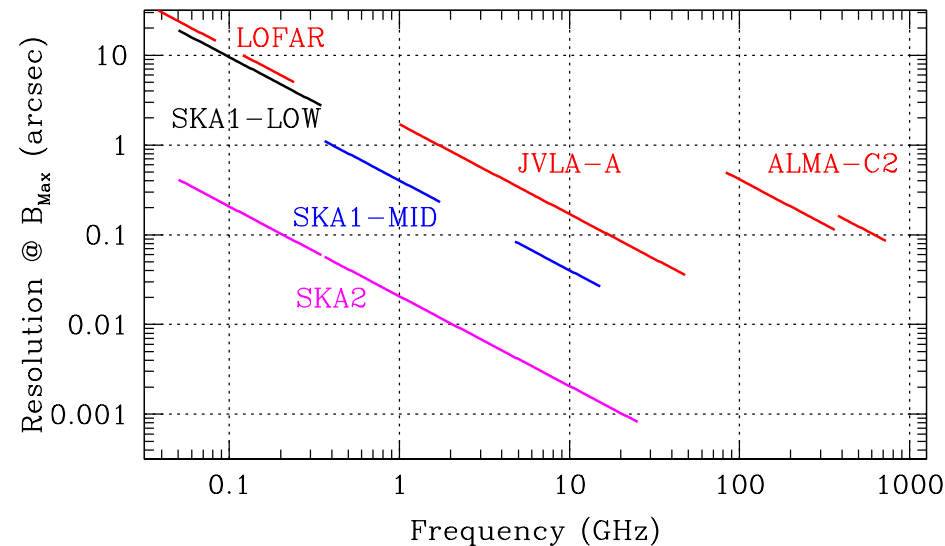
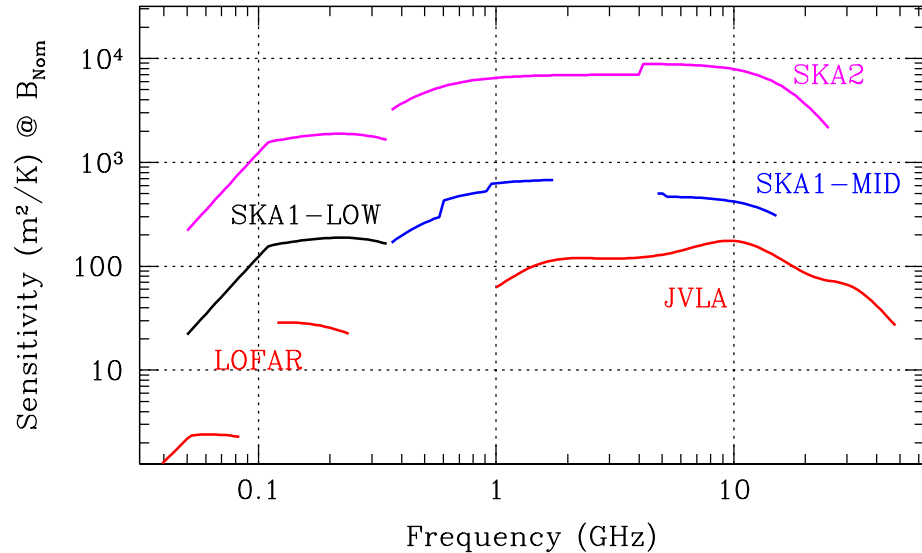
### ❖ Shallower slope ( $\alpha \sim -0.5$ ) of Stokes I at 22-408 MHz

- Free-free absorption is significant ( $\tau > 1$ ); absorption of synchrotron (I, Q, U)  $\propto e^{-\tau}$

$$\tau = 8.235 \times 10^{-2} T^{-1.35} \nu^{-2.1} EM \quad (\text{e.g. Waelkens et al. 2008})$$

- Temperature: H $\alpha$  observation

$$T_e(R, z) = 5780 + 287R - 526|z| + 1770z^2 \quad [\text{K}] \quad (\text{Paladini+ 04})$$



## ❖ Sensitivity

- 9000PSR+1400MSP (SKA1)
- 30000PSR+3000MSP (SKA2)
- QSOs ~ 200,000,000 (SKA2)
- dense RM grids / rare objects

## ❖ Angular resolution

- ~1" (baseline/60km)<sup>-1</sup>  
(frequency/1GHz)<sup>-1</sup>

## ❖ Bandwidth

- 0.1 - 25 GHz, 64k ch./band
- spectral index / depolarization/  
Faraday tomography

## ❖ FoV and Image quality

- x 100 survey speed of JVLA (SKA1)
- x 10<sup>4-6</sup> of JVLA (SKA1)
- A+B+C+D+E+A<sup>+</sup>

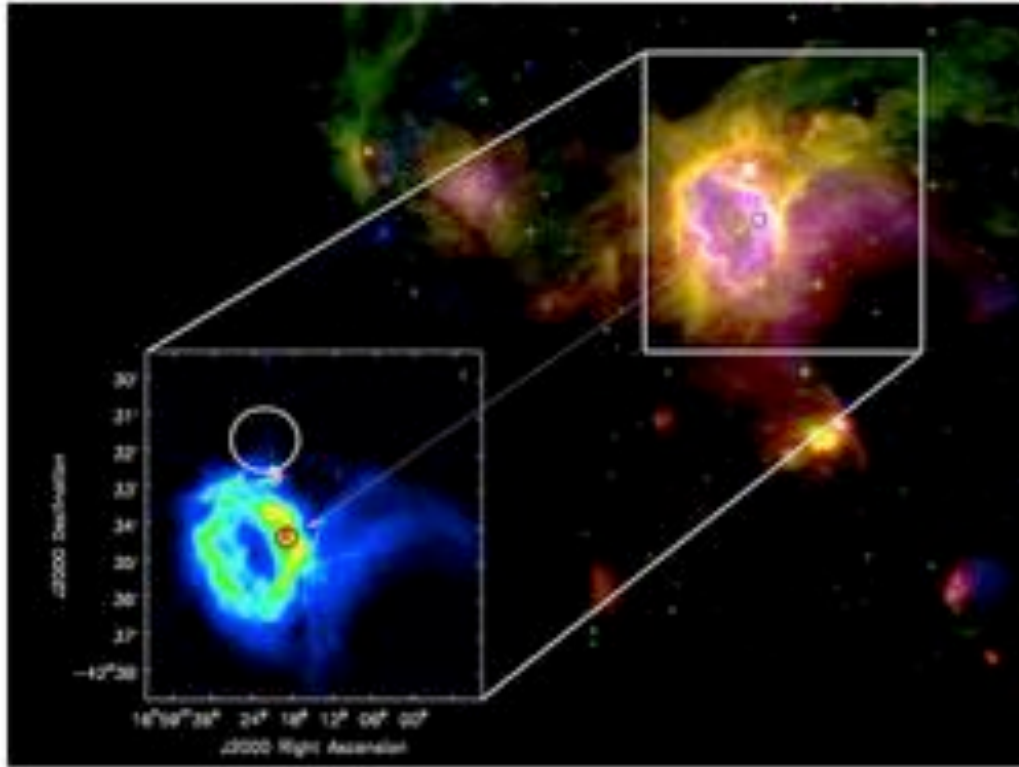
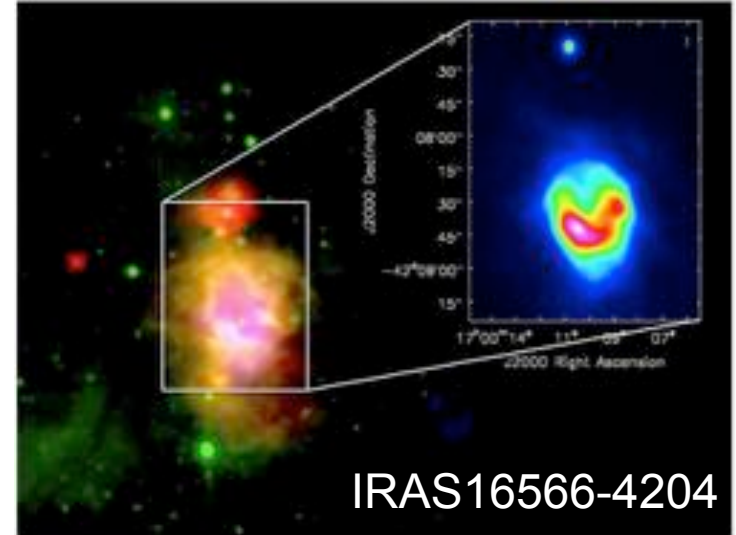
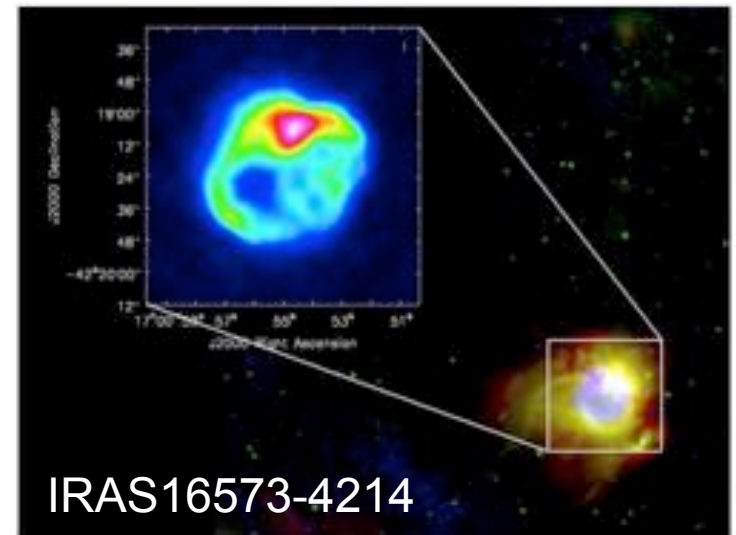


**Figure 5.** Composite picture of the field centred on [DBS2003] 176. The sub-panel shows only the SCORPIO map, while in the background panel the mid-IR/FIR maps from Spitzer (IRAC, 8 μm, green) and Herschel (PACS, 70 μm, red) are superimposed on the SCORPIO map, in blue. The white arrow indicates the position of the compact component SCORPIO1\_300. The white circle points out that there is no radio emission associated with S16 (see text).



IRAS16566-4204

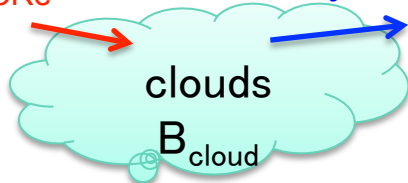


IRAS16573-4214

## ❖ Dense molecular clouds are bright at centimeter

– Gives field strength & orientation

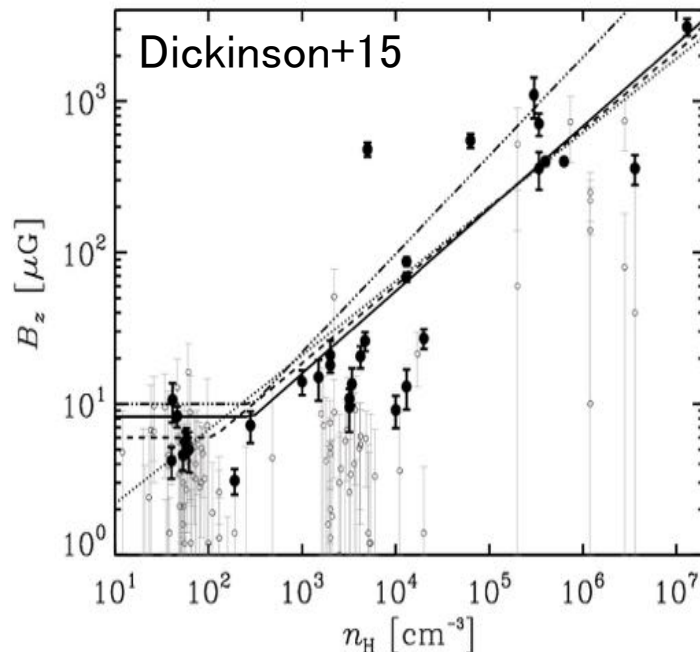
primary  $n_{\text{CRe}}$



$n_{\text{CRe}}$ : Strong+11,  $\gamma \sim 3$ ,  $\alpha \sim -1$

$B_{\text{cloud}}$ : Crutcher+10,  $B_z \propto n_{\text{H}}^\kappa$ ,  $\kappa \sim 0.6$

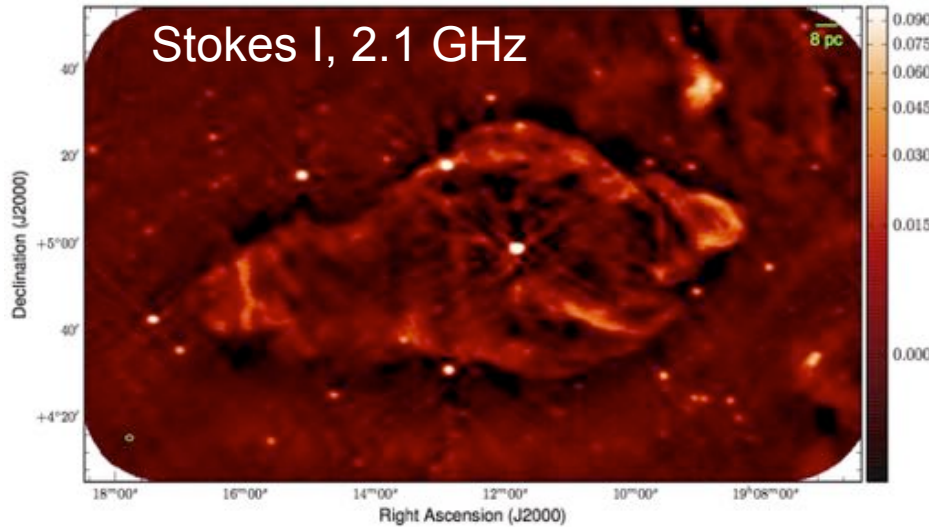
$$\left(\frac{S_{\text{pred}}}{\text{mJy}}\right) = 6.6 \times 10^6 \left(\frac{\Omega_{\text{src}}}{\text{sr}}\right) \left(\frac{N_{\text{H}}}{10^{23} \text{ cm}^{-2}}\right) \left(\frac{n_{\text{H}}}{300 \text{ cm}^{-3}}\right)^{\kappa(\gamma+1)/2-1}$$



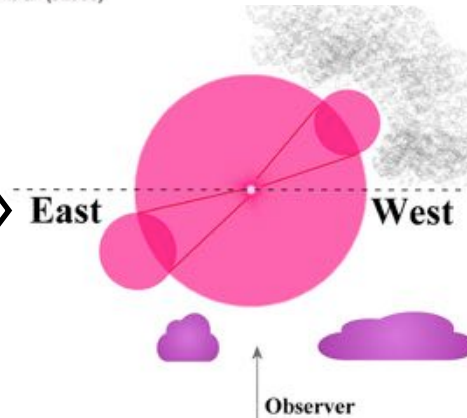
## O(0.1-1) mJy @ 1 GHz (5''~0.25pc @ 1kpc)

Name	$B_z$ [μG]	$n_{\text{H}_2}$ [cm <sup>-3</sup> ]	$R$ [pc]	$D$ [kpc]	$\theta$ [arcsec]	$T_{\text{GHz}}$ [mK]	$S_{\text{GHz}}$ [mJy]
W3 OH	3100	$6.31 \times 10^6$	0.02	2.0	4.0	0.06	0.05
DR21 OH1	710	$2.00 \times 10^6$	0.05	1.8	11.2	0.30	0.27
Sgr B2	480	$2.51 \times 10^3$	22.0	7.9	1149	1200	1000
M17 SW	450	$3.16 \times 10^4$	1.0	1.8	236	31	27.0
W3 (main)	400	$3.16 \times 10^5$	0.12	2.0	24.3	0.49	0.43
S106	400	$2.00 \times 10^5$	0.07	0.6	48.1	0.74	0.65
DR21 OH2	360	$1.00 \times 10^6$	0.05	1.8	11.2	0.14	0.13
OMC-1	360	$7.94 \times 10^5$	0.05	0.4	50.3	2.3	2.0
NGC2024	87	$1.00 \times 10^5$	0.2	0.4	196	14.6	13.0
W40	14	$5.01 \times 10^2$	0.05	0.6	34.4	0.04	0.03
$\rho$ Oph 1	10	$1.58 \times 10^4$	0.03	0.1	91.7	0.14	0.13

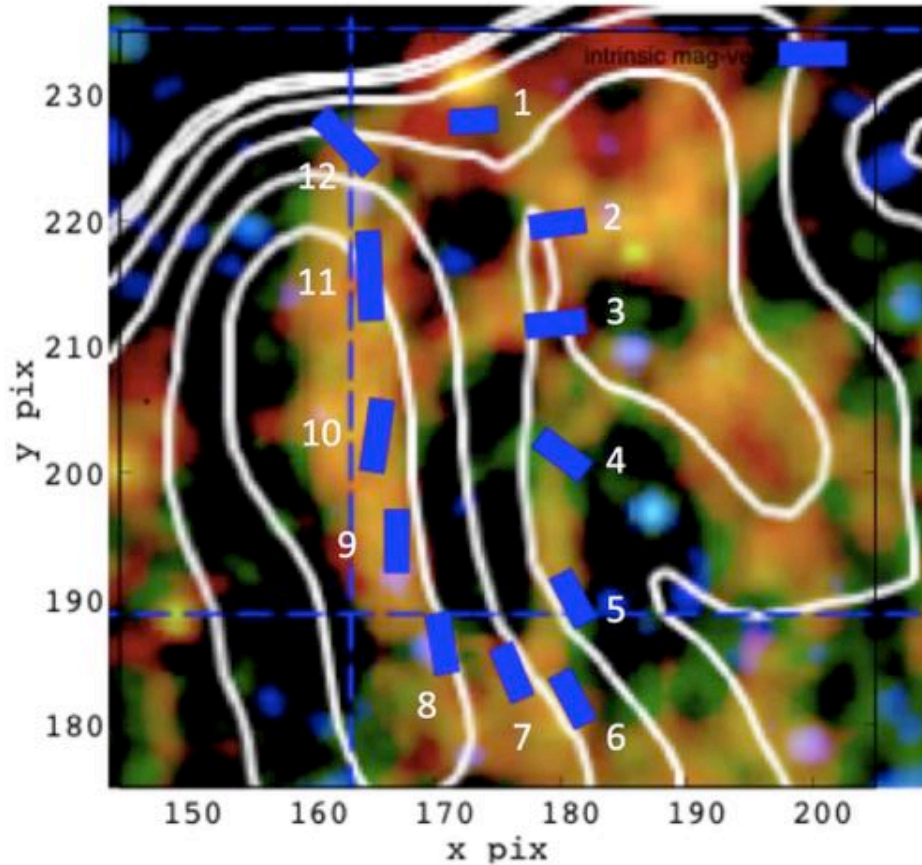
## ❖ “Manatee” Nebula W50



- Stokes I
- Stokes QU
- RM ( $\Phi$ )
- H $\alpha$  EM
- pulsar DM



Farnes, TA+ (2016) (1604.06552)



X-ray + magnetic field vector  
Sakemi et al. (in preparation)

## ❖ Diffuse Ionized Gas (DIG) in the Galaxy

- Sophisticated model of thermal electron density (DM, EM, SM)
- ASS/BSS disk + halo toroidal + vertical field (DM, EM, RM)
- Magnetic turbulence (EM, RM, I, P)
- Cosmic-ray electrons (I, P)

## ❖ Toward Square Kilometer Array (SKA)

- **High sensitivity, high resolution, wide band, wide field**
- Continuum mapping of star-forming regions & clouds
- High resolution imaging of Jet terminal region (shocks, lobes)